Experiment and analysis of the seed suction model for rice pneumatic seed metering device using DEM-CFD approach

He Xing[1,3], Yuwan Wang[2], Yuanbing Chen[2], Ru Yang[2], Xizhu Bo[1], Ying Zang[3*]

(1. *School of Information Technology & Engineering, Guangzhou College of Commerce, Guangzhou 511363, China*;
2. *School of Modern Information Industry, Guangzhou College of Commerce, Guangzhou 511363, China*;
3. *College of Engineering, South China Agricultural University, Guangzhou 510642, China*)

Abstract: The model describing the forces acting on rice seeds within seed metering systems significantly impacts the design and structural parameters of rice pneumatic seed metering mechanisms. To formulate a mathematical representation of the device during seed suction, a DEM-CFD bidirectional coupling approach was utilized to simulate and model the seed-suction process. The dynamic behavior of rice seeds under the airflow at the suction port was examined, and force models for various seed-suction positions were developed. Simulation analyses were conducted under varying conditions, including different rotation speeds of the seed-suction plate and different levels of negative suction pressure. The effects of these variables on seed suction were investigated, leading to the development of a drag force model. Optimal seeding parameters and precision were determined from the simulation results. Verification and analysis were conducted through empirical experiments, and the optimal seeding performance was attained at a negative suction pressure of 1.6 kPa and a plate rotation speed of 30 r/min. The results indicated a seeding qualification rate of 95.7%, a reattachment rate of 2.4%, and a leakage suction rate of 1.9%. The simulation findings were consistent with experimental data, demonstrating that the seed-metering device satisfies the requirements for field seeding.

Keywords: rice seeding, seed metering device, seed suction model, agricultural machinery, DEM-CFD
DOI: 10.25165/j.ijabe.20251805.9422

Citation: Xing H, Wang Y W, Chen Y B, Yang R, Bo X Z, Zang Y. Experiment and analysis of the seed suction model for rice pneumatic seed metering device using DEM-CFD approach. Int J Agric & Biol Eng, 2025; 18(5): 191–197.

1 Introduction

Rice is a crucial economic crop globally. Pneumatic rice seed metering devices facilitate direct field sowing. Compared to traditional mechanical counterparts, these pneumatic devices offer lower damage rates and higher precision in seeding, leading to their widespread use. Rice seeds, generally spindle-shaped with low sphericity, pose adsorption challenges, unlike more spherical seeds, which impacts suction precision and field application effectiveness of the pneumatic metering devices. Thus, a thorough analysis of the seed-suction model in these devices is essential to optimize their performance[1-3].

To elucidate the interaction between rice seeds and airflow during the operation of pneumatic metering devices, researchers globally have developed models for various types of these devices. Li et al.[4] constructed a mathematical model for constrained seed-suction conditions, focusing on the interaction between seeds and airflow in the flow field. Ding et al.[5,6] investigated the seed-suction posture of corn pneumatic seed metering devices using DEM-CFD coupled simulation technology, and analyzed key factors influencing seed suction, cleaning, and ejection. They established a negative pressure seed-suction model under different parameters to determine optimal operational settings, aiding the structural optimization of corn pneumatic seed metering devices. Shi et al.[7] developed a pneumatic seed metering device to facilitate auxiliary seed filling. The DEM-CFD gas-solid coupling method was employed to analyze factors affecting seed filling at various stages, and experiments were conducted to assess seed suction stability and seed removal resistance, resulting in an interaction model of these parameters. To enhance the effectiveness of corn pneumatic seed metering devices, Han et al.[8] used EDEM-CFD simulations to study the device's operation, optimizing the air nozzle position to increase the seeding qualification rate. Gao et al.[9] improved the pipeline structure of an air-blown seed metering device utilizing a Venturi pipeline and applied gas-solid coupling simulations to examine how different pipeline structures and airflow speeds impact seed transport. Zhang et al.[10] explored the functioning of hole-type seed metering devices, defining the filling dynamics between seeds and holes, and introduced a secondary seed-filling chamber, which was experimentally validated to obtain optimal structural parameters. Xing et al.[11-12] optimized the seed stirring mechanism in rice pneumatic seed metering devices, developed a stress model for rice seeds under agitation, and tested various stirring parameters to improve seeding precision. Yao et al.[13] designed a centralized pipeline system for rape pneumatic seed metering devices, and it was optimized through gas-solid two-way coupling and field validation to determine the best high-speed operation parameters. Wang et al.[14-16] developed a pneumatic seed metering device for wheat by using airflow ejection and blade propeller. Xu et al.[17]

Received date: 2024-10-14 **Accepted date:** 2025-06-11
Biographies: He Xing, PhD, Associate Professor, research interest: agricultural mechanization and automation, Email: hexing@scau.edu.cn; **Yuwan Wang**, Master, research interest: agricultural mechanization and automation, Email: 20210209@gcc.edu.cn; **Yuanbing Chen**, Master, research interest: agricultural mechanization and automation, Email: 3234231842@qq.com; **Ru Yang**, Master, research interest: agricultural mechanization and automation, Email: 923760103@qq.com; **Xizhu Bo**, PhD, research interest: agricultural mechanization and automation, Email: 20220474@gcc.edu.cn.
***Corresponding author: Ying Zang**, PhD, Professor, research interest: agricultural mechanization and automation. College of Engineering, South China Agricultural University, Guangzhou 510642, China. Tel: +86-20-38676975, Email: yingzang@scau.edu.cn.

designed a pneumatic seed metering device for vegetables, and optimized the seed-sucking plate parameters using computational fluid dynamics and discrete element methods. The experimental analysis clarified the internal flow field dynamics of the suction hole, and the seed-sucking model was validated through practical tests. Wu et al.[18] employed the BPM and MFBD-DEM coupled approach to develop an agglomerate model for rapeseed particles, analyzing their crushing characteristics and the forces exerted on flexible components, thereby providing a theoretical basis for the structural optimization of seeding machinery. Tang et al.[19,20] designed a pneumatic seed metering device for corn, formulated a theoretical model for seed suction, transport, and ejection, and optimized structural and negative pressure parameters through experiments to provide a basis for precise corn sowing technology. Cao et al.[21] investigated the irregular shape of Ning-guo Radix Peucedani seeds, designed a corresponding seed metering device, and used Rocky DEM simulations to analyze seed movement and establish a damage model meeting agronomic requirements. Dong et al.[22] studied a rice seed selection device, developed a selection platform, and analyzed the interaction of seeds with the wind field during filling. The DEM-CFD coupling method was utilized to understand the relationships among inlet wind speed, section shape, and distance, which offers a theoretical basis for seed selection.

Currently, research on gas-solid coupling modeling for pneumatic seed metering devices has primarily targeted crops like corn and rape. Due to the spindle shape, low sphericity, and high roughness of rice seeds, modeling studies specific to rice seeds are limited in pneumatic seed metering devices. This paper aims to investigate the movement mechanism of rice seeds during the seed-sucking process in a pneumatic rice seed metering device. Using the Rocky-Fluent coupling simulation method, a gas-solid coupling model was established to describe the interaction between rice seeds and the airflow at the suction hole. The optimal seeding performance was verified through practical seeding tests.

2 Working principle and seed-sucking model of rice pneumatic seed metering device

2.1 Working principle of rice pneumatic seed metering device

As shown in Figure 1, the rice pneumatic seed metering device includes a seed chamber shell, a suction chamber shell, a seed-sucking plate, a seedbox, and a seeding shaft, among other components. Throughout the functioning, rice seeds move from the seed container into the seed-sucking zone within the seed chamber shell. The seeds are then directed inside the device. The seed-sucking plate and suction chamber shell together form an air chamber. A vacuum pump creates negative pressure airflow, evacuating air from the air chamber through a pipeline, resulting in a vacuum. This generates negative pressure at the suction holes on the seed-sucking plate, causing rice seeds to adhere to these holes. The seeding shaft rotates the seed-sucking plate, carrying the attached seeds out of the seed-sucking zone, across the seed-carrying zone, and into the seed-dispensing zone. In this area, positive pressure air stream blows the seeds off the plate. With the assistance of gravity and positive pressure airflow, the seeds are ejected from the device and deposited into the field, thus completing the seeding process.

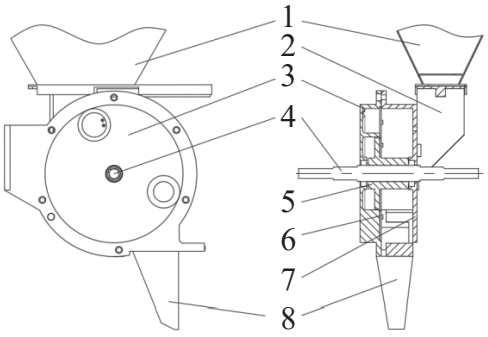

1. Seedbox 2. Seedbox connector 3. Sucking chamber shell 4. Seeding shaft 5. Flange 6. Seed-sucking plate 7. Seed chamber shell 8. Seeding tube

Figure 1 General structure diagram of rice pneumatic seed metering device

2.2 Rice seed-sucking force model of rice pneumatic seed metering device

As depicted in Figure 2, rice seeds experience various forces in distinct regions, necessitating an analysis of their stress models at different positions. Due to the low-speed movement and small size of rice seeds, air resistance is minimal and thus disregarded in the seed-sucking process. Rice seeds are influenced by forces from different planes, and their force analysis is performed in two planes. In the plane parallel to the seed-sucking plate, when rice seeds are initially adsorbed in the seed-sucking area, they remain within the seed population, indicating an accumulation state. There was a force of mutual extrusion between the seed population and a friction force between the seed population, and the synthesized force was F_s. At the same time, the rice seeds were also subjected to the gravity G, the centrifugal force F_r, and the supporting force F_j of the seed stirring device. When the rice seeds left the seed-sucking area along with the suction holes, the adsorbed rice seeds were separated from the seed population, formed an adsorption stable state under the action of the seed stirring device and the negative pressure sucking force, and synchronously rotated along with the seed-sucking plate. As the adsorbed rice seeds left the seed population, the force of the seed population on the adsorbed rice seeds disappeared, that is, F_s = 0, but other forces were still present. Through the above analysis, the force analysis is carried out in the plane parallel to the seed-sucking plate, and all the above forces are vector synthesized; the synthesized force was Q [11], and the expression is Equation (1):

$$Q = G + F_s + F_r + F_j \quad (1)$$

where, G is gravity of the rice seed, N; Q is combined force, N; F_s is friction between rice seeds, N; F_r is centrifugal force on rice seed, N; F_j is force of seed stirring device on rice seed, N.

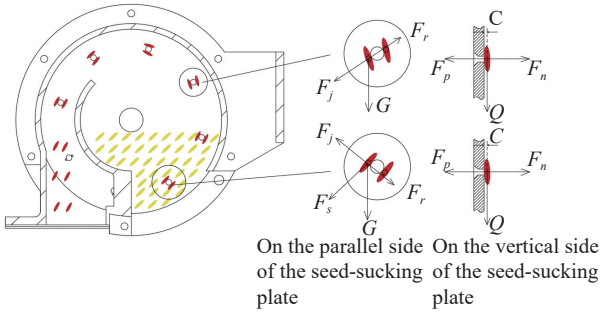

Figure 2 Force diagram of suction seed

In the direction perpendicular to the plane of the seed-sucking plate, the rice seeds were subjected to the sucking force F_p of the suction holes and the elastic force F_n of the seed-sucking plate on the seeds. According to the research results of Li[4], when the seed-sucking force was at the minimum, the seed-sucking plate did not produce an elastic force on the seeds, that is, F_n = 0. At this time, the suction force F_p was the limit seed-sucking force, as expressed

in Equation (2):

$$F_p \frac{d}{2} = QC \tag{2}$$

where, C is distance from the center of gravity of the rice seed to the row of seed-sucking plate, m; F_p is suction force on rice seeds, N; d is the diameter of the suction hole of the seed-sucking plate, m.

3 Modeling and analysis of seed-sucking simulation

3.1 Seed-sucking model of seed metering device

To determine the adsorption state and suction force of rice seeds at various positions within the seed metering device, coupling simulations were conducted using discrete element Rocky software and ANSYS-Fluent software. A seed suction force model was established, and the precision of seed-sucking was evaluated.

SolidWorks was employed to create the seed metering device model. Since the analysis focused on the seed-sucking force model, only the seed box channel, seeding chamber shell, seed-sucking plate, and suction chamber shell were included, resulting in a simplified model. This model was imported into Rocky software, and its schematic is illustrated in Figure 3a. Ansys-Workbench was used for meshing the flow field, defining the fluid inlet, outlet, and interface according to operational conditions. The meshed model was then imported into Fluent software. Suction holes were designated as the dynamic area, while other parts were set as static. The grid diagram is depicted in Figure 3b.

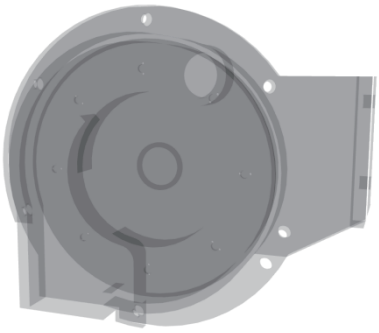

a. Seed metering device model in rocky

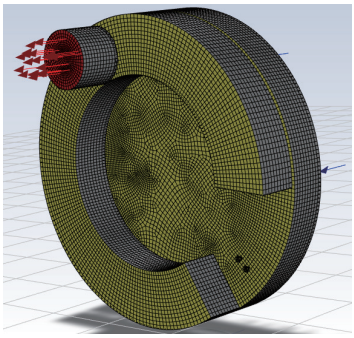

b. Mesh diagram in fluent

c. Simulated rice seed diagram

Figure 3 Seed metering device model, fluid mesh diagram, and simulated rice seed diagram

The seeds flowed into the seeding chamber shell from the seed box through the seed box channel and accumulated in the seed-sucking chamber. WUFENYOU 615 rice seeds were selected for experimental analysis in this paper to simulate the actual accumulation state of rice seeds. Through the measurement of the triaxial parameters of rice seeds in the early stage, the average triaxial dimensions of length, width, and thickness were 8.4 mm×2.2 mm×1.8 mm (l×w×t). The rice seed particle parameters in Rocky were set to be similar to the actual rice seed parameters, and the simulated rice seed is shown in Figure 3c.

3.2 Mathematical model for coupled simulation

The process of seed suction in a pneumatic rice seed expeller involves the dynamic interaction between airflow and rice seeds, focusing on the kinematic relationship between air and particles. This study employs the CFD-DEM gas-solid coupling approach for analysis.

The gas phase is treated as a continuous phase, following the principles of mass and energy conservation. Due to the low velocity of the particles, lift effects are ignored, with the main influence being the drag force exerted by the airflow during coupling. The two-phase coupling is described by the Navier-Stokes equations[23,24]. The governing equations for the continuous phase and the momentum conservation for the fluid phase are provided, with the fundamental equations detailed in Equations (3)-(7):

$$\frac{\partial(\varepsilon_g \rho_g)}{\partial t} + \nabla \cdot \varepsilon_g \rho_g u_g = 0 \tag{3}$$

$$\frac{\partial(\varepsilon_g \rho_g u_g)}{\partial t} + (\nabla \cdot \varepsilon_g \rho_g u_g u_g) = -\varepsilon_g \nabla p - S_p - (\nabla \cdot \varepsilon_g \tau_g) + \varepsilon_g \rho_g g \tag{4}$$

$$\tau_g = \mu[\nabla u_g + (\nabla u_g)^{-1}] \tag{5}$$

$$S_p = \frac{\sum F_{p,f}}{V_{\text{cell}}} \tag{6}$$

$$\varepsilon_g = 1 - \frac{\sum V_p}{V_{\text{cell}}} \tag{7}$$

where, ε_g is the void volume fraction; τ_g is the fluid viscous stress tensor, Pa; μ is the aerodynamic viscosity, Pa·s, and t is the time, s; S_p is the source term for the momentum exchange between particles and fluid, N/m³; V_{cell} is the cell volume, m³.

In the CFD-DEN coupled analysis, the dynamics of particles need to satisfy Newton's second law and Equations (8) to (11) need to be satisfied for the motion and rotation of any particle[25]:

$$m_p \frac{\mathrm{d}u_p}{\mathrm{d}t} = m_p g + F_{p,f} + F_{p,n} + F_{p,t} \tag{8}$$

$$I_p \frac{\mathrm{d}\omega_p}{\mathrm{d}t} = T_t + T_r + T_n \tag{9}$$

$$F_{p,f} = F_d - V_p \nabla p \tag{10}$$

$$F_d = 0.5 C_D \rho_g A |u_g - u_p| (u_g - u_p) \tag{11}$$

where, m_p denotes the mass of the particle, kg; u_p represents the particle velocity, m/s; $F_{p,f}$ is the interaction force between particle and fluid, N; $F_{p,n}$ signifies the normal force on the particle, N; $F_{p,t}$ indicates the tangential force, N; I_p is the moment of inertia, kg·m²; ω_p is the angular velocity, rad/s; T_n is the torques of normal force, N·m; T_r is the rolling friction torque, N·m; T_t is the torques of tangential force, N·m; ∇p is pressure gradient, Pa/m; V_p is particle volume, m³; F_d is the drag force, N; and C_D represents the drag coefficient. The drag coefficient C_D is determined by combining correlations proposed by Wen and Yu[26], as utilized by Gidaspow, Bezburuah, and Ding[27]. The local fluid velocity at the particle's position is computed using the bilinear interpolation method (Hoomans, 2000)[28]. ρ_g is gas density, kg/m³; A is the windward area of the particle, m²; u_g is the gas velocity, m/s; u_p is the particle velocity, m/s.

3.3 Parameters of coupling simulation experiment

Based on previous research findings[12] and the actual field seeding conditions, the primary factors influencing seed-sucking precision are the rotational speed of the seed-sucking plate and the negative pressure during seed-sucking. Consequently, these two parameters were selected as experimental variables. In field seeding operations, the seeder's operating speed ranges from 0.5 to 0.8 m/s, corresponding to a seed-sucking plate rotational speed of approximately 30-50 r/min. Thus, the rotational speed of the seed-sucking plate was set between 20 and 50 r/min. Previous studies indicated that a seed-sucking pressure ranging from –1.2 to –2.0 kPa is appropriate for simulation experiments. The levels of the simulation test factors are presented in Table 1.

Table 1 Table of experimental factor levels

Level	Factors	
	A. Rotational speed of the seed-sucking plate/r·min^{-1}	B. Negative pressure on suction seed/kPa
1	20	1.2
2	30	1.6
3	40	2.0
4	50	-

To improve the authenticity of the simulation, the parameters of the rice and seed metering device in reference [29] were referred to, and the parameters are listed in Table 2. A particle factory was arranged inside that seeding chamber shell, the quality of the rice seed produced by the particle factory was set to be 10 g/s, the generation time was set to be 2 s, and 20 g of rice seeds were produced in total. According to the parameters of rice seeds, 20 g of rice seeds was about 1800, slightly less than the number of rice seeds accumulated in the actual seed metering device. The particle factory produced rice seeds that fell freely by gravity and accumulated inside the seeding chamber shell. The DEM-CFD coupling mode was set in Rocky, the 2-way Fluent coupling was adopted, and the drag force model was set as Haider & Levenspiel. The seeding precision of 80 hills in each group was collected for statistical analysis. Because the rotation speed of the seed-sucking plate was different during the simulation, the total simulation time was also different.

Table 2 Simulation experiment parameters

Parameter	Rice seeds	Material of seed metering device (steel)
Density (ρ_p) /kg·m^{-3}	1200	7800
Poisson's ratio	0.3	0.28
Young's modulus/MPa	181.5	75
Coefficient of restitution (with seeds)	0.3	0.5
Coefficient of sliding friction (with seeds)	0.56	0.4
Coefficient of rolling friction (with seeds)	0.15	0.02

During DEM-CFD coupling analysis, to maintain synchronization, the rotational speed of the seed-sucking plate in Rocky was aligned with that in Fluent. Due to the low negative pressure airflow and slow flow velocity in the seed metering device, the RNG k-ε turbulence model was selected in Fluent based on prior research, using a simple algorithm for solving. The seed metering device's negative pressure interface was configured as a pressure outlet with values of –1.2 kPa, –1.6 kPa, and –2.0 kPa. The inlet was set as a pressure inlet with a value of 0. Air pressure circulation occurred at the interface (INTERFACE), while other boundaries were defined as walls (Wall). Following initialization, Fluent data was saved in .dat format and imported into Rocky for coupling simulation.

4 Results and analysis

To validate the precision of the simulation experiments, a practical seeding experiment was conducted using identical factors and levels. These experiments took place at the JPS-12 Seeding Test Station within the Key Laboratory of Key Technology on Agricultural Machine and Equipment, Ministry of Education, at South China Agricultural University. The test setup is depicted in Figure 4. Given the high efficiency of the seeding process in the actual experiments, 250 hills/groups were sampled for each equipment group, with three repetitions. Data were analyzed in accordance with the national standard GB-T 6973-2005[30]. The probabilities of 1-3 sucked seeds per hill were taken as a qualified index, the probabilities of 0 sucked seeds per hill as a missing hill, and the probabilities of ≥4 sucked seeds per hill as a multiple-sucking index.

Figure 4 Diagram of test setup

The process of emulating is depicted in Figure 5a, with the drag force results from the simulation experiment shown in Figure 5b, the drag force effect diagram in Figure 5c, and the pressure gradient force diagram in Figure 5d. The drag force experiment results indicate that as the rotation speed of the seed-sucking plate increases, the drag force decreases. This is primarily because a higher rotating speed reduces the number of seeds being sucked, thereby decreasing the interaction force between the airflow and particles, which in turn lowers the drag force. The diagrams also reveal that the drag force and pressure gradient force on rice seeds adsorbed by the inner circles are greater than those on seeds adsorbed by the outer circles. This is mainly due to the fact that rice seeds in the outer circles are influenced by the seed-stirring device during the seed-sucking process, providing some supportive force. Conversely, rice seeds in the inner circles, located beneath the seed-stirring device, do not receive such support. Therefore, the drag and pressure gradient forces on rice seeds in the inner circles are higher than those on the outer circles.

The precision results of the seeding simulations are depicted in Figure 6, while Figure 7 illustrates the outcomes of the actual seeding experiments. According to the simulation, the optimal seed-sucking effect occurred at a pressure of 1.6 kPa and a rotation speed of 30 r/min. Under these conditions, the seeding qualified rate was 92.5%, with a 5% probability of 0 seeds sucked per hill and a 2.5% probability of ≥4 seeds sucked per hill. When the seed-sucking pressures were set at 1.2, 1.6, and 2.0 kPa, the average probabilities of ≥4 seeds sucked per hill were 0.63%, 3.75%, and 9.69%, respectively, while the average probabilities of 0 seeds sucked per hill were 12.81%, 5.94%, and 1.25%. In the actual seeding experiments, the best performance was also achieved at a seed-

sucking pressure of 1.6 kPa and a rotation speed of 30 r/min, with a seeding qualified rate of 95.03%. The probability of 0 seeds sucked per hill was 2.17%, and the probability of ≥4 seeds sucked per hill was 2.80%. At seed-sucking pressures of 1.2, 1.6, and 2.0 kPa, the average probabilities of ≥4 seeds sucked per hill were 1.55%, 2.56%, and 7.06%, respectively, and the average probabilities of 0 seeds sucked per hill were 7.22%, 4.04%, and 1.55%.

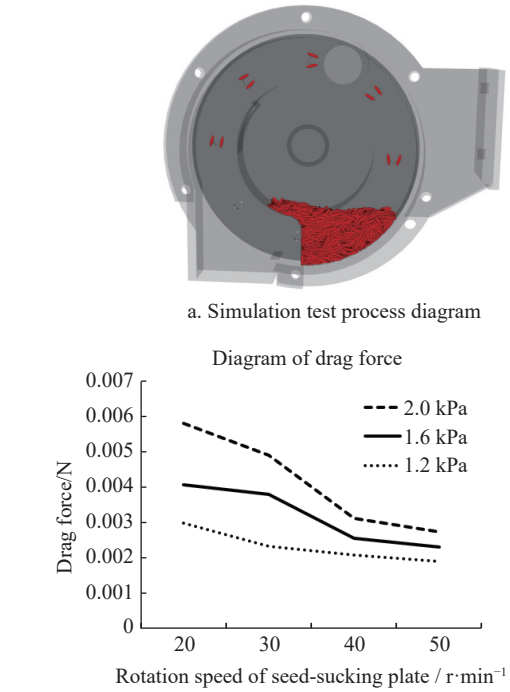

a. Simulation test process diagram

b. Plot of traction results diagram

c. Traction effect diagram

d. Pressure gradient force effect

Figure 5 Simulation test result graph

The findings from both the simulations and real-world experiments showed that an enhancement in the negative pressure of seed sucking enhances the quantity of seeds sucked, the average number of seeds per suction, and the probability of 4 or more seeds per hill. This is because higher negative pressure boosts the suction force at the holes, improving seed adsorption efficiency. Conversely, reducing the negative pressure decreases the likelihood of 4 or more seeds per hill, but increases the probability of 0 seeds per hill due to the weaker suction force, making stable seed-sucking more challenging.

It is evident that an increase in the rotational speed of the seed-sucking plate leads to a decrease in the overall seeding volume and an increase in the rate of empty holes. Simulation results for rotational speeds between 20-50 r/min show average cavity rates of 4.58%, 5.42%, 7.50%, and 9.17%, and average resorption rates of 7.50%, 4.17%, 4.17%, and 2.92%, respectively. Actual test results for the same speed range indicate average cavity rates of 2.28%, 2.69%, 5.18%, and 6.94%, with average resorption rates of 6.31%, 4.14%, 2.59%, and 1.86%. The primary reason for this is that higher rotational speeds reduce the time suction holes spend in the seed suction area, thereby diminishing interaction time between the suction holes and rice seeds, which adversely affects seed adsorption. Additionally, increasing rotational speed would result in higher centrifugal forces on the adsorbed seeds, reducing adsorption stability. These factors combined lead to an increased rate of empty holes and a decreased resorption rate with higher rotational speeds of the seed-sucking plate.

The variance analysis outcomes for both the theoretical simulations and real-world experiments are presented in Tables 3 and 4. In the simulation studies, the rotation speed of the seed-sucking plate significantly impacted the probabilities of 0 seeds per hill, while the negative pressure substantially affected both the probabilities of 0 seeds and ≥4 seeds per hill. Similarly, in the actual experiments, both the rotation speed of the seed-sucking plate and the negative pressure had a notable effect on these probabilities. The variance results from the simulations were consistent with those from the actual experiments. Thus, the negative pressure and rotation speed are identified as the primary factors influencing the probabilities of 0 seeds and ≥4 seeds per hill.

The consistency between the actual and simulation experiment results confirms their reliability. Comparing both sets of results under identical conditions revealed that the qualified rate in the simulations was lower than in the actual experiments. This discrepancy is primarily due to the smaller quantity of rice seeds

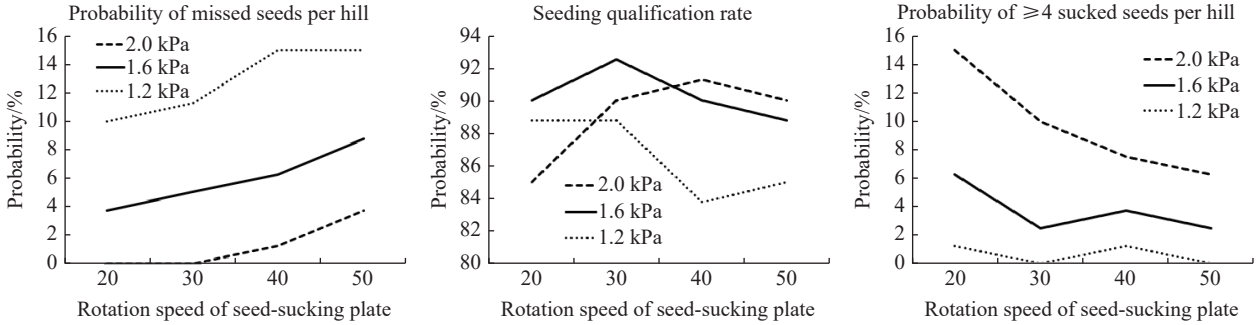

Figure 6 Seeding precision results of simulation test

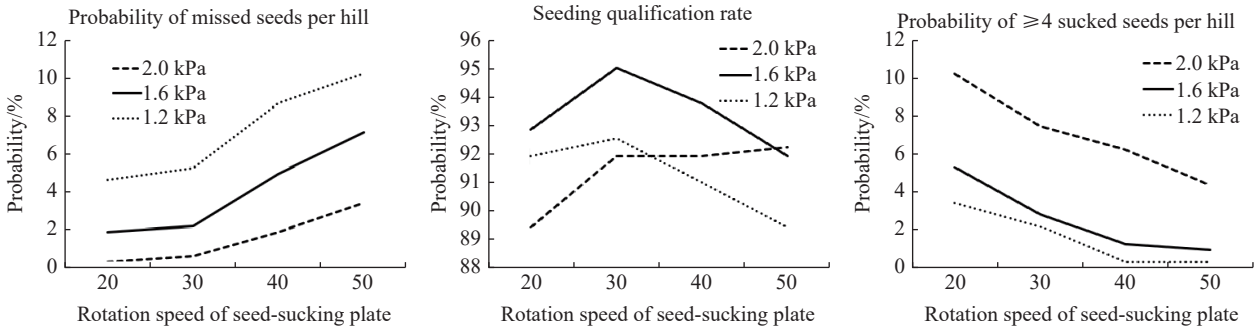

Figure 7 Seeding precision results of actual test

used in the simulations to expedite the process. With fewer seeds, the time the suction holes spend in the seed suction area is reduced, resulting in less interaction time for effective seed adsorption. Consequently, the actual experiments demonstrated better performance than the simulations.

Table 3 Analysis of variance (Simulation experiment)

Analysis	Missed seeds per hill		≥4 sucked seeds per hill/%		1-3 sucked seeds per hill/%	
	A	*B*	*A*	*B*	*A*	*B*
SS	0.004	0.027	0.003	0.017	0.001	0.003
df	3	2	3	2	3	2
MS	0.001	0.014	0.001	0.008	0.000	0.001
F	17.412	183.353	3.296	24.111	0.687	2.333
Sig	0.002	0.000	0.100	0.001	0.592	0.178
Significance	**	**		**		

Note: ** is significant (p<0.01). The same below.

Table 4 Analysis of variance (Actual experiment)

Analysis	Missed seeds per hill		≥4 sucked seeds per hill/%		1-3 sucked seeds per hill/%	
	A	*B*	*A*	*B*	*A*	*B*
SS	0.004	0.006	0.003	0.007	0.001	0.001
df	3	2	3	2	3	2
MS	0.001	0.003	0.001	0.003	0.000	0.001
F	26.990	60.558	30.809	91.213	1.677	4.097
Sig	0.001	0.000	0.000	0.000	0.270	0.076
Significance	**	**	**	**		

5 Discussion

Based on the findings from both simulations and actual experiments, the primary reason for the discrepancies observed is the insufficient quantity of rice seeds used in the simulation experiments for the seed metering device. This insufficiency resulted in a reduced seed-sucking area and inadequate time for the seed-sucking plate to engage with the seeds, negatively impacting the adsorption efficiency of the suction holes. Additionally, the lower number of rice seeds led to decreased extrusion forces among the rice seeds, the seeding chamber shell, and the seed-sucking plate. Consequently, most of the adsorbed seeds were those directly in contact with the seed-sucking plate, forming a layer tightly attached due to the extrusion force from outer seeds, thereby increasing friction and aiding adsorption. With fewer seeds, this extrusion force diminished, thus reducing adsorption effectiveness in simulations compared to actual experiments.

In the simulation analysis of this study, no impurities were included since the rice seeds were modeled under ideal conditions as steel bodies, which did not incur damage from interactions with the seed-stirring device. However, in practical scenarios, rice seeds contain various impurities. When these seeds interact with the stirring device, there is a likelihood of damage, leading to husk detachment. The husks, having lower mass than the seeds, are more readily adsorbed by the suction holes, reducing the seed-sucking efficiency of the device. Prolonged operation can cause these impurities to block some suction holes, further affecting adsorption. Future simulations should incorporate impurities and model rice seeds as non-steel bodies to better reflect actual conditions.

To mitigate the impact of impurities during field seeding, repeated cleaning of rice seeds to reduce impurity content is recommended. Additionally, using flexible materials for the seed-stirring device can minimize friction and collision, minimizing seed damage and preventing husk detachment.

Simulation experiments only considered the friction parameters between rice seeds and the seed metering device, without accounting for the awns on rice seed surfaces. These awns affect seed movement and interaction with suction holes. Due to the limited research on rice seed micro-surfaces, accurate modeling remains challenging. Future research should focus on micro-surface modeling to enhance simulation accuracy.

6 Conclusions

This study employed the DEM-CFD fluid-solid coupling method to model and analyze the seed-suction process of a pneumatic rice seed metering device. The interaction between the seed-sucking plate and rice seeds was examined through simulation software, and subsequent analyses and experiments were performed. The simulation results indicated that optimal seed-sucking performance occurred at a pressure of 1.6 kPa and a seed-sucking plate rotation speed of 30 r/min, which yielded a qualified seeding rate of 92.5%, 5% probability of 0 seeds sucked per hill, and 2.5% probability of ≥4 seeds sucked per hill. To validate these simulation results, experiments were conducted under identical conditions. The experimental findings confirmed that at 1.6 kPa pressure and 30 r/min rotation speed, the best seed-sucking effect was achieved, with a qualified seeding rate of 95.03%, a 2.17% probability of 0 seeds sucked per hill, and a 2.80% probability of ≥4 seeds sucked per hill. The consistency between simulation and actual experimental results confirmed the reliability of the simulation, satisfying the criteria for field seeding.

Acknowledgements

The authors are thankful for funding from the National Natural Science Foundation of China (Grant No. 32201669), the Guangzhou Science and Technology Plan Project (Grant No. 2023A04J0865), Key Discipline Research Capability Enhancement Project in Guangdong Province (Grant No.2024ZDJS081) ,Guangdong Provincial Junior Innovative Talents Project for Ordinary Universities (Grant No. 2022KQNCX122), the project was

supported by Open Fund of State Key Laboratory of Agricultural Equipment Technology, South China Agricultural University (Grant No.SKLAET-202405), Guangzhou College of Commerce Campus Project (Grant No. 2021XJYB06), and Guangdong Provincial Key Laboratory of Agricultural Artificial Intelligence Open Plan Project (Grant No. GDKL-AAI-2022002; GDKL-AAI-2022003).

[References]

[1] Min H, Sheng L F, Fang B C, Jiang C, Shuang L S, Yu L, et al. Early sowing increases grain yield of machine-transplanted late-season rice under single-seed sowing. Field Crops Research, 2020; 253: 107832.

[2] Ke L, Rui Y, Jun D, Li Y H, Zhong W W, Guo H M, et al. High radiation use efficiency improves yield in the recently developed elite hybrid rice Y-liangyou 900. Field Crops Research, 2020; 253: 107804.

[3] Blümmel M, Duncan A J, Lenné J M. Recent advances in dual purpose rice and wheat research: A synthesis. Field Crops Research, 2020; 253: 107823.

[4] Li L. A preliminary study on the theory and experimentation of the suction-type metering device for precision drill. Transactions of the CSAM, 1979; 10: 56–63. (in Chinese).

[5] Li D, Ye C Y, Yu F D, Chen X L, Zhan H, Guang M G, et al. Design and experiment of air-suction maize seed-metering device with auxiliary guide. Agriculture, 2024; 14: 169.

[6] Ding L, Yang L, Zhang D X, Cui T, Zhang K L, Zhong X J. Effect of seed adsorption posture of corn air-suction metering device on seed feeding performance. Transactions of the CSAM, 2021; 52(7): 40–50.

[7] Shi S, Liu H, Wei G J, Zhou J L, Jian S C, Zhang R F. Optimization and experiment of pneumatic seed metering device with guided assistant filling based on EDEM CFD. Transactions of the CSAM, 2020; 51(5): 54–66.

[8] Dan D H, Wei L, Yu N W, Qing W, Zhi J W, Yu C W, et al. CFD-DEM coupling analysis of the negative pressure inlet structural parameters on the performance of integrated positive-negative pressure seed-metering device. Frontiers in Plant Science, 2025; 16: 1485710.

[9] Xiao J G, Guan F X, Jiang L, Guang S, Qing H L, Yu X H. Design and validation of a centrifugal variable diameter pneumatic high-speed precision seed metering device for maize. Biosystems Engineering, 2023; 227: 161–181.

[10] Zhang M H, Wang Z M, Luo X W, Zang Y, Yang W W, Xing H, et al. Review of precision rice hill-drop drilling technology and machine for paddy. Int J Agric & Biol Eng, 2018; 11(3): 1–11.

[11] He X, Xiao M Cao, Peng Z, Yi K W, Jun J L, Yu Z, et al. DEMCFD coupling simulation and optimisation of rice seed particles seeding a hill in double cavity pneumatic seed metering device. Computers and Electronics in Agriculture, 2024; 224: 109075.

[12] He X, Zai M W, Xi W L, Si Y H, Ying Z. Mechanism modeling and experimental analysis of seed throwing with rice pneumatic seed metering device with adjustable seeding rate. Computers and Electronics in Agriculture, 2020; 178: 105697.

[13] Yao X, Zi T M, Ming L W, Hai F L. Numerical study of pneumatic conveying of rapeseed through a pipe bend by DEM-CFD. Agriculture, 2022; 12: 1845.

[14] Ying B W, Meng Z H, Qiu H Y, Zeng W Z. DEM-CFD simulation and seed orientation evaluation of a self-suction wheat shooting device. Powder Technology, 2023; 427: 118746.

[15] Ying B W, Hong W L, Hong N H, Jin H, Qing J W, Cai Y L, et al. DEM-CFD coupling simulation and optimization of a self-suction wheat shooting device. Powder Technology, 2021; 393: 494–509.

[16] Ying B W, Hong W L, Hong N H, Qing J W, Cai Y L, et al. A noncontact self-suction wheat shooting device for sustainable agriculture: A preliminary research. Computers and Electronics in Agriculture, 2022; 197: 106927.

[17] Jian X, Shun L S, Zhao K H, Xiao M W, Zhi H Z, Jie L, et al. Design and optimisation of seed-metering plate of air-suction vegetable seed-metering device based on DEM-CFD. Biosystems Engineering, 2023; 230: 277–300.

[18] Wu W C, Deng X, Li J, Hu J F, Cheng H, Zhou W, et al. Micro-level stress characteristics of rapeseed particle during the seeding process using the MFBD-DEM coupled method. Computers and Electronics in Agriculture, 2024; 220: 108929.

[19] Han T, Fu D X, Tian Y G, Chang S X, Jin W W. Design and test of a pneumatic type of high-speed maize precision seed metering device. Computers and Electronics in Agriculture, 2023; 211: 107997.

[20] Han T, Chang S X, Zi M W, Qi W, Jin W W. Optimized design, monitoring system development and experiment for a long-belt finger-clip precision corn seed metering device. Frontiers in Plant Science, 2022; 28: 814747.

[21] Cao C M, Ding W Y, Liu Z B, An M H, Zhang X C, Qin K. Design and Experiment of Seed Disperser for Ning-guo Radix Peucedani Based on Rocky Dem. Transactions of the CSAM, 2023; 54(8): 53–64.

[22] Hao D, Bao F Z, Tao J, Yi F Z, Ji W Q, Chao C, et al. Design and optimization of rice grain screening system based on DEM-CFD coupled rice seed testing platform. Agronomy, 2022; 12: 3069.

[23] Kafui K D, Thornton C, Adams M J. Discrete particle-continuum fluid modelling of gas–solid fluidised beds. Chem. Engng Sci, 2002; 57: 2395–2410.

[24] Kafui K D, Thornton C, Adams M J. Reply to comments by Feng and Yu on 'Discrete particle-continuum fluid modelling of gas-solid fluidised beds'. Chem. Engng Sci. 2004; 59: 723–725. DOI: 10.1016/j.ces.2003.11.004.

[25] Yong Z, Yu L D, Chang W, Yi C. Numerical simulation of hydrodynamics in downers using a CFD-DEM coupled approach. Powder Technol, 2010; 199: 2–12.

[26] Wen C Y, Yu Y H. Mechanics of fluidization. Chemical Engineering Progress Symposium Series, 1966; 62: 100–111.

[27] Gidaspow D, Bezburuah R, Ding J. Hydrodynamics of circulating fluidized beds: Kinetic theory approach. In O. E. Potter, & D. J. Nicklin (Eds.), Fluidization VII (pp.75–82). New York: Engineering Foundation. 1991.

[28] Bob P B H. Granular dynamics of gas–solid two-phase flows (Doctoral dissertation). 2000. Netherlands: Universiteit Twente.

[29] Liu C L, Wang Y L, Song J N, Li Y N, Ma T. Experiment and discrete element model of rice seed based on 3D laser scanning. Transactions of the CSAE, 2016; 32(15): 294–300.

[30] GB/T 6973-2005: Testing method for single seed drills (precision drills). Beijing, China: Chinese National Standards. China, 2005. (in Chinese).